PRINT ISSN 1119-8362
Electronic ISSN 2659-1499

Full-text Available Online at
https://www.ajol.info/index.php/jasem
https://www.bioline.org.br/ja

J. Appl. Sci. Environ. Manage.
Vol. 28 (4) 1053-1060 April 2024

Terminalia catappa Leaf Extract as a Capping Agent for ZnO Nanoparticle Synthesis via Sol-gel Method and its Microbial Effects on Selected Fungi and Bacterial

[*1]JAJI, SB; [1]OCHIGBO, SS; [2]ABUBAKAR, AY; [3]SULEIMAN, MAT; [3]OKAFOR, JO; [4]OLUTOYE, AF

[1]Department of Chemistry, Federal University of Technology, Minna, PMB 65, Minna, Niger State, Nigeria*
[2]Department of Biochemistry, Ibrahim Badamasi Babangida University Lapai, Niger State, Nigeria
[3]Department of Chemical Engineering, Federal University of Technology, Minna, PMB 65, Minna, Niger State, Nigeria
[4]Department of Biochemistry, University of Ilorin, Kwara State, Nigeria

**Corresponding Author Email: jajibola36@gmail.com*
**ORCID: https://orcid.org/0009-0003-4843-0739*
**Tel:+2348035348778*

Co-Authors Email: stephen.ochigbo@gmail.com; awwaluinyass@gmail.com; smatsule@yahoo.com; jo.okafor@futminna.edu.ng; olutoyeabdulquadri@gmail.com

ABSTRACT: This study presents a reliable process for synthesizing ZnO nanoparticles using a green method. In this approach, we harness *Terminalia catappa* leaf extract as an effective chelating and capping agent to synthesize ZnO nanoparticles from zinc nitrate hexahydrate salt through a sol-gel method, employing Response Surface Methodology (RSM) and its microbial assessment. Optical properties of the ZnO nanoparticles were investigated using UV-visible spectroscopy, and determined their band-gap to range between 4.13 and 5.175 eV. To explore the outcomes, Response Surface Methodology (RSM), was employed which revealed that the Model F-value of 2.62 signifies the significance of the model for the response. Furthermore, when examining the contour plot relating the inhibition zone to temperature and plant extract dosage, we found that an increase in dosage and decrease in temperature resulted in an increase in the bandgap. This method of biosynthesizing zinc oxide nanoparticles through *Terminalia catappa* leaf extract offers effect against the bactieria and fungi such as; *Escherichia -coli, Straphylococcus aureus, Pseudomonas aeuginosa* and *Trichophyton rubrum, Penicillium marnaffei, Atteneria spp* respectively. Therefore, ZnO nanoparticles though this route gives an eco-friendly and more straightforward alternative to chemical and physical synthesis techniques for various environmental applications.

DOI: https://dx.doi.org/10.4314/jasem.v28i4.6

Cite this Article as: JAJI, S. B; OCHIGBO, S. S; ABUBAKAR, A. Y; SULEIMAN, M. A. T; OKAFOR, J. O; OLUTOYE, A. F. (2024). Terminalia catappa Leaf Extract as a Capping Agent for ZnO Nanoparticle Synthesis via Sol-gel Method and its Microbial Effects on Selected Fungi and Bacterial. *J. Appl. Sci. Environ. Manage.* 28 (4) 1053-1060

Dates: Received: 22 January 2024; Revised: 29 February 2024; Accepted: 23 March 2024 Published: 14 April 2024

Keyword: *Terminalia catappa*, sol-gel method, bandgap, response surface methodology, eco-friendly

Nanotechnology stands as a pivotal technology for the future, and in recent years, its significance has grown in the realm of nanomaterial development. Nanotechnology is the discipline focused on creating, analyzing, and utilizing structures measuring less than 100 nanometers (nm) in at least one dimension (Findik, 2021). Nanomaterials like SiO2, Fe_2O_3, ZnO, TiO_2, and others are commonly referred to as nanoparticles due to their inherent characteristics. Biosynthetic nanotechnology boasts an array of applications and the size reduction of materials leads to the emergence of novel physicochemical properties and a wide spectrum of potential uses (Pillai *et al.*, 2020; Mathew *et al.*, 2024). ZnO possesses a higher refractive index and

**Corresponding Author Email: jajibola36@gmail.com*
**ORCID: https://orcid.org/0009-0003-4843-0739*
**Tel:+2348035348778*

prominent UV light features. The characteristics of ZnO nanoparticles rely on the precise control of both physical and chemical properties, including size, size disparity, shape, surface state, crystal structure organization, and dispersibility (Demir *et al.*, 2023). ZnO has drawn considerable research interest due to its extensive range of applications, including UV sensors (Alamdari *et al.*, 2019; Inobeme *et al.*, 2023), targeted drug delivery (Anjum et al., 2021), antioxidant activity (Muthuvel *et al.*, 2020), biosensors (Shetti *et al.*, 2019; Adetunji et al., 2022), and environmental remediation (Qamar *et al.*, 2020; Mathew *et al., 2023*). One remarkable aspect of nanoparticle biosynthesis is the ability to selectively control the morphology of the resulting nanoparticles based on the biological source used, enhancing their stability. Biological synthesis methods employ either plant extracts or microbes to facilitate nanoparticle formation (Jeevanandam et al., 2022). Green practices exhibit several characteristics that render them more significant than chemical processes. A major advantage lies in the potential applications of biosynthesized nanoparticles in the biomedical field, stemming from their reduced toxicity compared to those produced via physicochemical methods.

The antimicrobial activity of the ZnO nanoparticles acted against various bacteria reveals distinct effectiveness across different materials, potentially influenced by the types and concentrations of ions present. ZnO nanoparticles likely to release zinc ions (Zn^{2+}), known for their antimicrobial properties. Another advantage may be the stabilizing effects of the biocomponents used in the synthesis process. Among the various biological methods, plant-mediated synthesis holds appeal due to features such as feasibility, the use of readily available plants, and the wide variety of ZnO nanoparticle morphologies (Tran *et al*., 2023). For examples, Jayachandran *et al*. (2021) observed the UV-visible spectrometer absorption peak of ZnO at 320 nm, which the average size of the nanoparticles of 52.24 nm. Also, Barzinjy and Azeez (2020) reported the UV-vis analysis of *Eucalyptus globulus* leaf extract for biosynthesized ZnO nanoparticles. They confirmed the spherical-shape of the ZnO with an average size between 27 and 35 nm with the band-gap of 2.67 eV.

Based on our previous efforts related to the synthesis of nanoparticles and investigation about their bio-applications, this study intended to synthesize ZnO-NPs with plant extract of *Terminalia catappa*. In this work, a simple, cost-effective, and green synthesis of ZnO nanoparticles was carried out using response surface methodology (RSM). Characterization of the nanoparticles for optical properties was also evaluated.

MATERIALS AND METHODS

Sample Preparation and Extraction: Zinc nitrate used for the synthesis was purchased from Sigma Aldrich. The plant used in the study was *Terminalia catappa* and the leaves were collected from Federal University of Technology, Bosso Campus, Minna, Niger State, Nigeria. All preparations were carried out by using double-deionized water. The plant extract was prepared by adding 10 g of *Terminalia catappa* leaf powder to 1000 cm^3 of de-ionized water in a 1000 cm^3 capacity beaker. The mixture was heated at 80 ^oC for 2 h on a magnetic stirrer. The extract obtained after heating was cooled and filtered first using mucilin cloth, then with Whatman filter paper No.1. A brown colour filtrate was obtained as leaf extract and was used as capping/stabilizing agent for the synthesis of the nanoparticles. The extract was stored in a glass bottle and kept in the refrigerator for the synthesis of ZnO nanoparticles.

Synthesis of ZnO-NPs: The volume of extract was added to 50 cm^3 of 0.5 M of zinc acetate dihydrate solution in a 250 cm^3 beaker. The mixture was stirred with magnetic stirrer with continuous stirring time. 0.5 M sodium hydroxide was added drop-wise to the solution on a continuous mixture to obtain the desired pH. A precipitate was obtained and later filtered by Whatman No. 1 filter paper. The precipitate obtained was washed with deionized water and ethanol to eliminate traces of the unreacted precursors. The final product was oven-dried at 105 ^oC for 24 h and finally calcined in the furnace to obtain ZnO nanoparticles.

Characterization: UV–vis spectral analysis was recorded on a double-beam spectrophotometer to ensure the formation of ZnO nanoparticles.

Optimization design and statistical analysis: The production and optimization of ZnO NPs biosynthesis were carried out using Response Surface Methodology (RSM). To assess the impact of independent variables, a Box-Behnken design (BD) was utilized, which encompassed 29 experiments, including the central point (Table 1). The independent variables encompassed stirring time (in minutes), volume of extract (in cubic centimeters), pH, and temperature (in degrees Celsius). The Design-Expert software (Version 13, State-Ease, Inc., Minneapolis, MN, USA) was employed for designing and analyzing the experimental data and for generating 3D plots to determine the optimal synthesis of ZnO-NPs with respect to the bandgap (in electronvolts,eV).

Antimicrobial activity of ZnO Nanoparticles: Antimicrobial activities of ZnO nanoapticle against bacteria and fungi were evaluated by the agar well-diffusion method by (Murray *et al.*, 1995) and minimum inhibitory concentration (MIC).

Agar Well-diffusion Method: The agar well-diffusion method was followed to determine the antimicrobial activity. Nutrient agar (NA) and Potato Dextrose Agar (PDA) plates were swabbed (sterile cotton swabs) with eight-hour-old broth cultures of the respective bacteria and fungi. Wells (10 mm diameter and about 2 cm apart) were made in each of these plates by using a sterile cork borer. The ZnO nanoparticle was prepared at a concentration of 1 mg/ml. About 100 µl of different concentrations of the ZnO nanoparticle were added with a sterile syringe into the wells and allowed to diffuse at room temperature for two hours. Control experiments comprising inocula without ZnO nanopaticle were set up. The plates were incubated at 37°C for 18-24 hours for bacterial pathogens, and at 28°C for 48 hours for fungal pathogens. The diameter of the inhibition zone (mm) was measured and the activity index was also calculated (Olurinola *et al.*, 1996).

Table 1. Experimental design variables with the predicted and actual results of bandgap on biosynthesized ZnO nanoparticles

Run	Stirring time (min)	Volume of extract (cm3)	pH	Temperature (°C)	Bandgap (eV) Actual	Bandgap (eV) Predicted
1	60	55	6	350	4.471	4.488
2	30	55	9	500	4.727	4.840
3	30	55	9	200	4.749	4.784
4	60	70	9	350	4.536	4.718
5	60	55	9	500	4.942	4.970
6	45	40	9	500	4.952	4.957
7	45	55	9	350	4.448	4.917
8	45	70	6	350	4.493	4.422
9	45	55	6	500	4.843	4.745
10	30	55	12	350	4.757	4.628
11	30	55	6	350	4.133	4.278
12	45	40	6	350	4.698	4.667
13	45	70	12	350	4.478	4.573
14	45	55	9	350	5.042	4.917
15	45	55	9	350	5.101	4.917
16	45	70	9	500	5.233	5.175
17	45	55	12	200	4.407	4.553
18	60	55	12	350	4.529	4.272
19	45	55	6	200	4.392	4.430
20	45	40	12	350	4.515	4.649
21	45	55	9	350	4.881	4.917
22	45	70	9	200	4.654	4.538
23	60	40	9	350	4.595	4.674
24	45	40	9	200	5.13	5.077
25	45	55	12	500	4.744	4.755
26	45	55	9	350	5.115	4.917
27	60	55	9	200	4.558	4.508
28	30	40	9	350	5.086	4.952
29	30	70	9	350	4.617	4.586

RESULTS AND DISCUSSION

UV-visible analysis: Results of UV–visible spectroscopy, as shown in Fig. 1, unveiled a distinct peak at 275 nm, a characteristic feature of ZnO nanoparticles (NPs). This peak was attributed to the phenomenon of surface plasmon resonance (SPR), and the sharpened nature of the peak served as compelling evidence of the successful synthesis of monodisperse ZnO NPs.

Generally, ZnO NPs exhibit an absorption peak maximum within the range of 300 to 380 nm. Notably, the assessed value, at 275 nm, is lower than that of bulk ZnO, typically reported as 240 nm (Fadillah *et al.*, 2019). This discrepancy indicates a blue shift in excitonic absorption, pointing to the occurrence of a small quantum confinement effect.

Optimization studies: The band-gap energy (Eg) of ZnO nanoparticles is determined by fitting the reflection data to the linear transformation formula $\alpha h\nu = A(h\nu - Eg)^n$. In this equation, α represents the optical-absorption parameter, hv stands for the energy of a photon, Eg is the band-gap energy, A is a constant, and the exponent n is dependent on the type of optical transition that prevails. Specifically, when n = 1/2, an optimal linearity is observed for the allowed transition. The specific value of the band-gap is calculated by extrapolating the linear portion of $(\alpha h\nu)^2$ versus hv to the x-axis. The band-gap energy for ZnO nanoparticles falls within the range of 4.133 to 5.233 eV, as indicated in Table 2. The optimization of biosynthesizing ZnO nanoparticles (NPs) using the Response Surface Methodology with Box-Behnken design (RSM-BD) is a valuable statistical and mathematical approach. This method effectively elucidates the influence of independent variables on various processes and their associations with the resulting outcomes by establishing a mathematical model. Based on the results obtained from the RSM analysis (Table 1), the bandgap ranged from 4.133 to 5.175 eV. To best represent the experimental data, a quadratic model for the size of ZnO NPs was selected, taking into account the main variable effects, curvature effects, and the interaction among factors. This model was chosen due to its high coefficient of determination ($R^2 = 0.7240$), a significant F-value (2.62), and a low lack of fit. The model is expressed as follows (see Eq. 1):

$$Y = +4.92 – 0.0365A – 0.0804B + 0.0332 + 0.1293D + 0.1025AB – 0.1415AC + 0.1015\ AB + 0.0420BC + 0.1893BD – 0.0285CD – 0.1728A^2 - 0.0119B^2 – 0.03278C^2 + 0.0310D^2 \quad (1),$$

where A is stirring time, B is volume of extract, C is pH and D is the temperature. In this model, the correlation coefficient (R2) value signifies a low level of agreement between experimental and predicted responses, suggesting a lack of model significance. Furthermore, the "p-value" was found to be less than 0.05, indicating the statistical significance of the model, with a p-value of 0.0409 for the bandgap value responses.

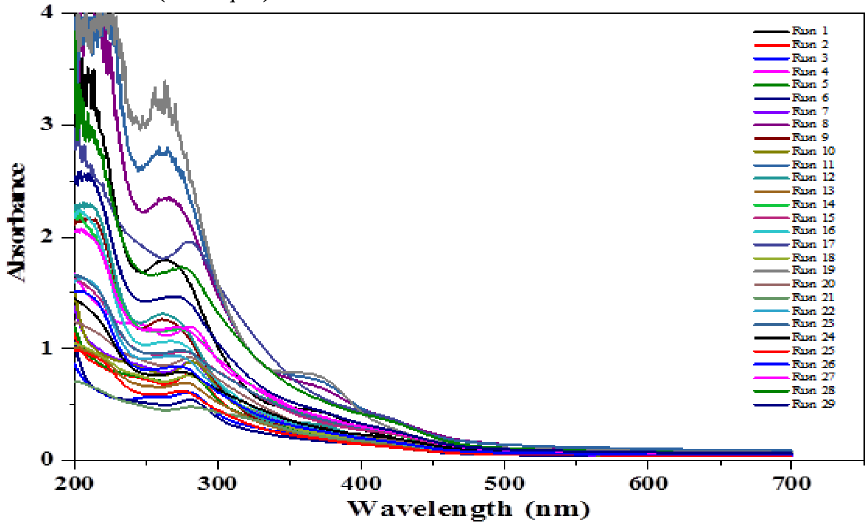

Fig. 1: UV-visible spectra of biosynthesized ZnO nanoparticles at different conditions

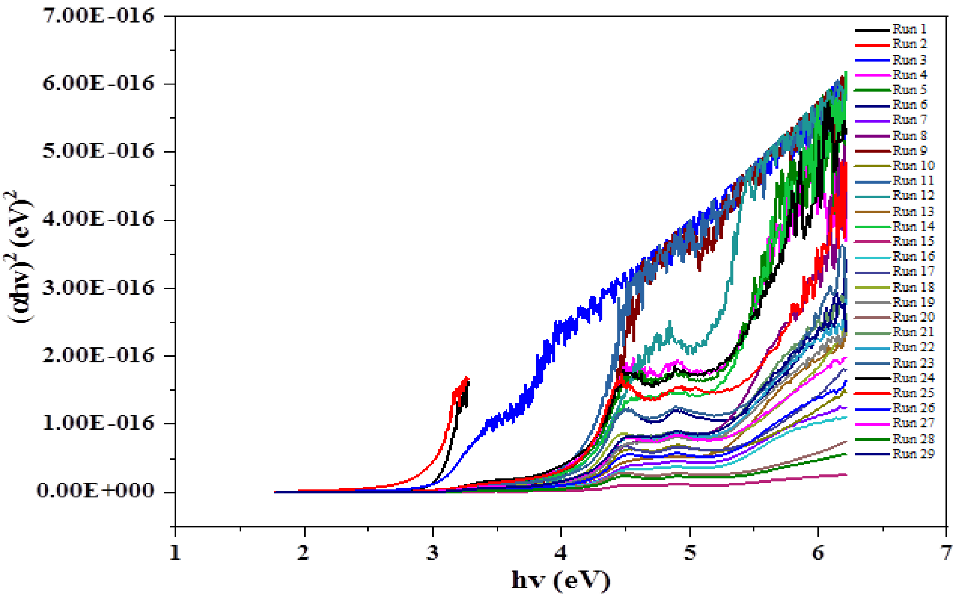

Fig. 2: Band gap energy (Tauc) plots of $(\alpha h\nu)^{1/2}$ versus $h\nu$ of biosynthesized ZnO nanoparticles

Table 2: The ANOVA for Quadratic model of biosynthesized ZnO nanoparticles

Source	Sum of Squares	df	Mean Square	F-value	p-value	
Model	1.51	14	0.1077	2.62	0.0409	significant
A-Stirring time	0.0160	1	0.0160	0.3893	0.5427	
B-Volume	0.0776	1	0.0776	1.89	0.1908	
C-pH	0.0133	1	0.0133	0.3247	0.5778	
D-Temperature	0.2005	1	0.2005	4.88	0.0443	
AB	0.0420	1	0.0420	1.02	0.3289	
AC	0.0801	1	0.0801	1.95	0.1843	
AD	0.0412	1	0.0412	1.00	0.3335	
BC	0.0071	1	0.0071	0.1718	0.6848	
BD	0.1433	1	0.1433	3.49	0.0829	
CD	0.0032	1	0.0032	0.0791	0.7826	
A^2	0.1937	1	0.1937	4.72	0.0475	
B^2	0.0009	1	0.0009	0.0226	0.8828	
C^2	0.6971	1	0.6971	16.98	0.0010	
D^2	0.0063	1	0.0063	0.1523	0.7022	
Residual	0.5749	14	0.0411			
Lack of Fit	0.2650	10	0.0265	0.3420	0.9231	not significant
Pure Error	0.3099	4	0.0775			
Cor Total	2.08	28				

R^2 = 0.7240, Adjusted R^2 = 0.4479, Predicted R^2 = 0.0347

The coefficient of variance (C.V. %) for the bandgap value response is calculated as 4.30% (as seen in Fig. 3). Fig. 4 depicts 3D and contour plots illustrating the interactions among the independent variables for both responses. The elliptical shapes of the curves clearly highlight significant interactions among these variables. Notably, an increase in the ZnO-to-extract ratio maximizes the bandgap in the biosynthesis of ZnO NPs. Additionally; stable NPs are produced at higher pH values due to the presence of numerous hydroxyl groups at higher pH levels, which can be oxidized with positively charged metal ions. This stability arises from the formation of a protective coating on the NP surface. The pH value plays a crucial role in the biosynthesis of metallic NPs. Changes in pH can lead to the alteration of biomolecules responsible for capping and stabilizing NPs (Bahari *et al.*, 2023). At higher pH values, protons and metal ions compete to bind to negatively charged regions, ultimately leading to increased biosynthesis of ZnO NPs under alkaline conditions.

As illustrated in Table 3, the absorption levels increase with higher extract amounts but decrease at elevated temperatures. When more charge carriers are present, there is a greater probability of absorption of photons with energy equal to or greater than the bandgap energy of the semiconductor. The bandgap absorption is a direct result of electrons in the valence band absorbing energy and transitioning to the conduction band, leaving behind holes. With more charge carriers, there is an enhanced chance of these absorption events occurring, leading to higher bandgap absorption. However, as the temperature continues to increase significantly, another effect comes into play, increased thermal scattering and phonon interactions. These interactions can disrupt the movement of charge carriers, reducing their mobility. At extremely high temperatures, these interactions can even cause electrons to lose energy and fall back into the valence band, effectively reducing the number of charge carriers available for absorbing photons.

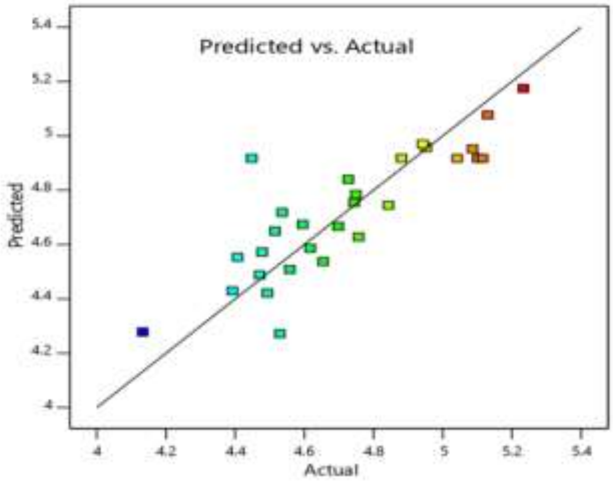

Fig. 3: Plot of Predicted versus experimentally observed values of bandgap on ZnO nanoparticles

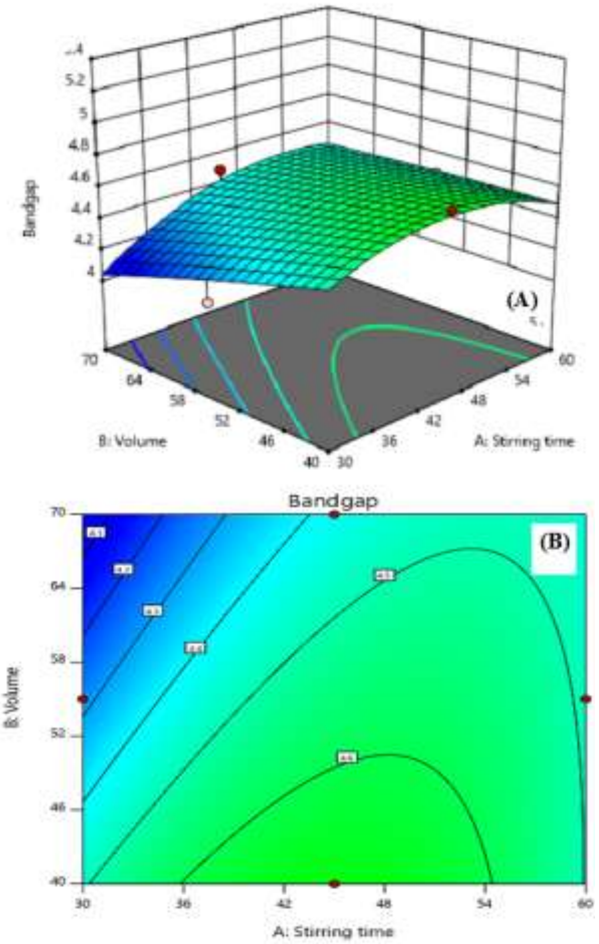

Fig. 4: (a) 3D Response surface interaction between volume extract and stirring time at a pH of 6 and **Fig 4 (b)** contour plot

The antimicrobial activity of the ZnO nanoparticles acted against various bacteria and fungi. The observed antimicrobial activity against *E. coli* suggests the efficacy of these ions against the fungus and bacterium.

Inhibition zone of 34.50 mm, indicate strong effectiveness against *E. coli*. However, for *Staphylococcus aureus*, only shows a mild zone 23.02 mm while pseudomonas demonstrates antimicrobial activity with an inhibition zone of 20.03 mm, (Filipović *et al.*, 2021).

The presence of specific ions in the ZnO nano could enhance its antimicrobial properties against *Staphylococcus aureus* and *Pseudomonas aeruginosa* as shown in Table 3.above. The antimicrobial activity of the ZnO against fungi reveals significant variations in effectiveness across different fungal species.

Among these species, *Trichophyton rubrum* shows the highest susceptibility The ZnO nanopaticle exhibits moderate activity with an inhibition zone of 9.00 mm, inhibition zone of 4.00 mm. For *Penicillium marnaffei*, release ions such as zinc (Zn^{2+}) ions, known for its antimicrobial properties (Sirajunisha *et al.*, 2023).

Factors such as surface morphology, porosity, and particle size may influence their antimicrobial properties.

Table 3. Bacterial and fungi analysis (Zone of inhibition)

ZnO nanooparticle				
S/N	Bacteria		Fungi	
1.	*Escherichia coli*	34.50mm	*Trichophyton rubrum*	9.00mm
2	*Staphylococcus aureus*	23.02	*Penicillium marnaffei*	35.50m
3	*Pseudomonas aeruginosa*	20.03	*Atterneria spp*	16.00mm

Conclusion: The utilization of *Terminalia catappa* leaf extract as an efficient chelating and capping agent for the synthesis of zinc oxide nanoparticles (ZnO NPs) through the sol-gel method, employing Response Surface Methodology (RSM), represents a significant advancement in the field of nanomaterial synthesis. This approach not only demonstrates the sustainable use of natural resources but also offers a precise and controlled means of producing ZnO NPs with tailored properties. The results obtained from this study clearly highlight the potential of *Terminalia catappa* leaf extract in facilitating the formation and stabilization of ZnO NPs. Moreover, the application of RSM ensures optimization of the synthesis process, enabling researchers to fine-tune various parameters to achieve the desired characteristics of the nanoparticles. This not only enhances the reproducibility of the synthesis but also promotes eco-friendliness and cost-effectiveness. The findings of this research have broad implications, with applications ranging from materials science to environmental engineering, catalysis, and biomedicine. The sustainable nature of the leaf extract-based synthesis approach and the precise control offered by RSM make it a promising avenue for the development of advanced nanomaterials for various industrial and scientific purposes.

REFERENCES

Adetunji, CO; Ogundolie FA; Ajiboye, MD; Mathew, JT; Inobeme, A; Olotu T; Olaniyan, O; Ijabadeniyi, OA; Ajayi, OO; Dauda, WP; Ghazanfar, S; Adetunji, JB. (2022). Bio- and Nanosensors in the Food Industry. In a book: Bio- and Nano-sensing Technologies for Food Processing and Packaging, The Royal Society of Chemistry, 22-36. doi:10.1039/9781839167966-00022

Alamdari, S; Ghamsari, M. S; Afarideh, H; Mohammadi, A; Geranmayeh, S; Tafreshi, M. J; Ehsani, M. H. (2019). Preparation and Characterization of GO-ZnO Nanocomposite for UV Detection Application. *Optic. Mater. 92*, 243-250.

Anjum, S; Hashim, M; Malik, S. A; Khan, M; Lorenzo, J. M; Abbasi, B. H; Hano, C. (2021). Recent Advances in Zinc Oxide Nanoparticles (ZnO NPs) for Cancer Diagnosis, Target Drug Delivery, and Treatment. *Canc.*, 13(18), 4570.

Bahari, N; Hashim, N; Abdan, K; Md Akim, A; Maringgal, B; Al-Shdifat, L. (2023). Role of Honey as a Bifunctional Reducing and Capping/Stabilizing Agent: Application for Silver and Zinc Oxide Nanoparticles. *Nan. Mater.* 13(7), 1244.

Barzinjy, A. A; Azeez, H. H. (2020). Green Synthesis and Characterization of Zinc Oxide Nanoparticles Using *Eucalyptus globulus* Labill. Leaf Extract and Zinc Nitrate Hexahydrate Salt. *SN Appl. Sci.*, 2(5), 991.

Demir, M; Özbay, E; Kamış, H; Haspulat Taymaz, B. (2023). Facile Fabrication of ZnO Nanoparticles for Efficient Dye Degradation: Effect of Adipic Acid in Photocatalytic Activity. *Che. Sel.*, 8(8), e202203822.

Fadillah, R; Rati, Y; Dewi, R; Farma, R; Rini, A. S. (2021). Optical and Structural Studies on Bio-Synthesized ZnO Using *Citrullus lanatus* Peel Extract. *In. J. of Phy. Conf. Ser.* 1816 (1). 012019.

Findik, F. (2021). Nanomaterials and their Applications. *Period. Engineer. Nat. Sci.*, 9(3), 62-75.

Filipović, V; Lončar, B; Knežević, V; Nićetin, M.; Filipović, J; Petković, M. (2023). Modeling the Effect of Selected Microorganisms' Exposure to Molasses's High-Smolality Environment. *Appl. Scie.*, 13(2), 1207.

Inobeme, A; Adetunji, CO; Ajai, AI; Inobeme, J; Mathew, JT; Obar, A; Maliki, M; Nwakife, N; Eziukwu, C. (2023). Chemical Nanosensors for Monitoring Environmental Pollution. In book: Advanced Application of Nanotechnology to Industrial Wastewater, Springer Nature Singapore, 93-103. doi: 10.1007/978-981-99-3292-4_6.

Jayachandran, A., Aswathy, T. R., Nair, A. S. (2021). Green Synthesis and Characterization of Zinc Oxide Nanoparticles Using *Cayratia pedata* Leaf Extract. *Biochem. and Biophy. Rep.*, 26, 100995.

Jeevanandam, J; Kiew, S. F; Boakye-Ansah, S; Lau, S. Y; Barhoum, A; Danquah, M. K; Rodrigues, J. (2022). Green Approaches for the Synthesis of Metal and Metal Oxide Nanoparticles Using Microbial and Plant Extracts. *Nan. Sca.*, 14(7), 2534-2571.

Mathew, J. T., Musah, M., Azeh, Y. & Muhammed, M. (2024). Development of Fe3O4 Nanoparticles for the Removal of Some Toxic Metals from Pharmaceutical Wastewater. Caliphate Journal of Science & Technology (CaJoST), 6(1), 26-34. DOI: https://dx.doi.org/10.4314/cajost.v6i1.4

Mathew, J. T., Musah, M., Azeh, Y. Muhammed, M. (2023). Adsorptive Removal of Selected Toxic Metals from Pharmaceutical Wastewater using Fe_3O_4/ZnO Nanocomposite, *Dutse Journal of Pure and Applied Sciences*, 9(4a), 236- 248. https://dx.doi.org/10.4314/dujopas.v9i4a.22.

Muthuvel, A; Jothibas, M; Manoharan, C. (2020). Effect of Chemically Synthesis Compared to Biosynthesized ZnO-NPs Using *Solanum nigrum* Leaf Extract and their Photocatalytic, Antibacterial and *In-vitro* Antioxidant Activity. *J. of Env. Chem. Eng*, 8(2), 103705.

Murray PR; Baron EJ; Pfaller MA; Tenover FC; Yolken HR. Manual of Clinical Microbiology. 6 th ed. Washington DC: ASM Press; 1995. p. 15-8.

Olurinola PF; A Laboratory Manual of Pharmaceutical Microbiology. Idu, Abuja, Nigeria: National Institute for Pharmaceutical Research and Development; 1996. p. 69-105.

Pillai, A. M; Sivasankarapillai, V. S; Rahdar, A; Joseph, J; Sadeghfar, F; Rajesh, K; Kyzas, G. Z. (2020). Green Synthesis and Characterization of Zinc Oxide Nanoparticles with Antibacterial and Antifungal Activity. *J. of Mol. Struc.*, 1211, 128107.

Qamar, M. A; Shahid, S; Javed, M. (2020). Synthesis of Dynamic g-C3N4/Fe ZnO Nanocomposites for Environmental Remediation Applications. *Ceram. Int'l*, 46(14), 22171-22180.

Shetti, N. P; Bukkitgar, S. D; Reddy, K. R; Reddy, C. V; Aminabhavi, T. M. (2019). ZnO-Based Nano Structured Electrodes for Electrochemical Sensors and Biosensors in Biomedical Applications. *Biosen. Bioelectron.* 141, 111417.

Sirajunisha, H; Balakrishnan, T; Sakthivel, P; Krishnaveni, A. (2023). Enhanced Corrosion Resistance, Antibacterial and Biological Properties of Sol-gel Derived Ti-rGO-HAp Nanocomposites. *Chem. Phy. Imp.*, 6, 100159.

Tran, G. T; Nguyen, N. T. H; Nguyen, N. T. T; Nguyen, T. T. T; Nguyen, D. T. C; Van Tran, T. (2023). Formation, Properties and Applications of Microalgae-Based ZnO Nanoparticles: A Rev. *J. of Envir. Chem. Eng.*, 110939.